Extremophiles (2016) 20:301–310
DOI 10.1007/s00792-016-0822-1

ORIGINAL PAPER

Genomic and physiological analysis reveals versatile metabolic capacity of deep-sea *Photobacterium phosphoreum* ANT-2200

Sheng-Da Zhang[1,3] · Claire-Lise Santini[2,3] · Wei-Jia Zhang[1,3] · Valérie Barbe[4] · Sophie Mangenot[4] · Charlotte Guyomar[2,3] · Marc Garel[5] · Hai-Tao Chen[1,3] · Xue-Gong Li[1,3] · Qun-Jian Yin[1,3] · Yuan Zhao[6] · Jean Armengaud[7] · Jean-Charles Gaillard[7] · Séverine Martini[5] · Nathalie Pradel[5] · Claude Vidaud[7] · François Alberto[2,3] · Claudine Médigue[8] · Christian Tamburini[5] · Long-Fei Wu[2,3]

Received: 23 December 2015 / Accepted: 1 March 2016 / Published online: 2 April 2016

Abstract Bacteria of the genus *Photobacterium* thrive worldwide in oceans and show substantial eco-physiological diversity including free-living, symbiotic and piezophilic life styles. Genomic characteristics underlying this variability across species are poorly understood. Here we carried out genomic and physiological analysis of *Photobacterium phosphoreum* strain ANT-2200, the first deep-sea luminous bacterium of which the genome has been sequenced. Using optical mapping we updated the genomic data and reassembled it into two chromosomes and a large plasmid. Genomic analysis revealed a versatile energy metabolic potential and physiological analysis confirmed its growth capacity by deriving energy from fermentation of glucose or maltose, by respiration with formate as electron donor and trimethylamine *N*-oxide (TMAO), nitrate or fumarate as electron acceptors, or by chemo-organo-heterotrophic growth in rich media. Despite that it was isolated at a site with saturated dissolved oxygen, the ANT-2200 strain possesses four gene clusters coding for typical anaerobic enzymes, the TMAO reductases. Elevated hydrostatic pressure enhances the TMAO reductase activity, mainly due to the increase of isoenzyme TorA1. The high copy number of the TMAO reductase isoenzymes and pressure-enhanced activity might imply a strategy developed by bacteria to adapt to deep-sea habitats where the instant TMAO availability may increase with depth.

Keywords Deep-sea adaptation · Bioluminescence · TMAO reductase · Hydrostatic pressure · Anaerobic respiration

Abbreviations

TMAO	Trimethylamine *N*-oxide
CDS	Coding DNA sequence

Introduction

Photobacterium are Gram-negative bacteria and represent one of the major genera of the family *Vibrionaceae*. This genus consists of about two-dozen validated species

Communicated by H. Atomi.

Electronic supplementary material The online version of this article (doi:10.1007/s00792-016-0822-1) contains supplementary material, which is available to authorized users.

✉ Long-Fei Wu
wu@imm.cnrs.fr

1 Deep-Sea Microbial Cell Biology, Department of Deep Sea Sciences, Sanya Institute of Deep-Sea Science and Engineering, Chinese Academy of Sciences, Sanya, China

2 LCB UMR 7257, Aix-Marseille Université, CNRS, IMM, 31, Chemin Joseph Aiguier, 13402 Marseille Cedex 20, France

3 France-China Bio-Mineralization and Nano-Structure Laboratory (LIA-BioMNSL), LCB-CNRS, Marseille, France/SIDSSE-CAS, Sanya, China

4 DSV/IG/Genoscope/LF, CEA, Evry, France

5 Aix-Marseille Université, Université du Sud Toulon-Var, CNRS/INSU, IRD, Mediterranean Institute of Oceanography (MIO), UM110, 13288 Marseille, France

6 Key Laboratory of Marine Ecology and Environmental Sciences, Institute of Oceanology, Chinese Academy of Sciences, Qingdao, China

7 DSV, iBEB/SBTN, CEA, Bagnols-sur-Cèze, France

8 Laboratoire d'Analyse Bioinformatique en Génomique et Métabolisme, CEA/DSV/IG/Genoscope and CNRS-UMR 8030 and Univ. Evry Val d'Esssone, Evry, France

(including subspecies) and more than 450 undefined species based on the 16S rRNA gene sequence analysis (see NCBI taxonomy website). They are facultative aerobes and derive energy from oxido-reduction of organic compounds. *Photobacterium* species are widespread in coastal, open-ocean and deep-sea environments, and occur in free-living form in seawater and sediments, or associated with marine animals. They function as decomposers of dead fish, pathogens for marine animals and human, or symbionts of light organs of fish and squid in the marine ecosystems. Seven *Photobacterium* species are luminous (Ast and Dunlap 2005). Three species, *P. kishitanii*, *P. leiognathi* and *P. mandapamensis* form bioluminescent symbioses with marine animals (Urbanczyk et al. 2011). Genetic attributes underpinning the eco-physiological adaptation remain poorly understood. Twelve *Photobacterium* genomes are available till now (Table 1), including piezophilic and piezosensitive *P. profundum* strains, which have been studied thoroughly for understanding the mechanism of bacteria adaptation to the high hydrostatic pressure. Eloe et al. have compared the two *P. profundum* genomes and found two sets of flagellar genes coding for lateral and polar flagella in the piezophilic strain SS9 but only the polar flagellar system in the piezosensitive strain 3TCK (Eloe et al. 2008). Similar dual flagellar systems have been reported for the deep-sea *P. profundum* DSJ4 (Campanaro et al. 2005). Moreover, synthesis of several terminal oxidases of anaerobic respiration in the piezophilic strain SS9 is up-regulated at high hydrostatic pressure (Campanaro et al. 2005; El-Hajj et al. 2010; Vezzi et al. 2005). The occurrence of dual flagellar systems and up-regulation of enzymes involved in energy metabolism have been proposed to be developed by deep-sea microbes to adapt to the high-pressure environments.

The *Photobacterium phosphoreum* strain ANT-2200 (hereafter called ANT-2200) was isolated at 2200 m depth from the Mediterranean Sea and capable of emitting bioluminescence (AlAli et al. 2010; Martini et al. 2013). Incubation at 22 MPa increases both its growth rate and light emission compared to cultures at atmosphere condition, indicating a moderately piezophilic feature (AlAli et al.

Table 1 Overview of *Photobacterium* genomes

Species	Strain	Assembly number (UID)	Size (Mbp)	GC (%)	Assembly level	No. of scaffolds	No. of contigs	Chrom./plasmid	No. of CDS	Isolated from
P. phosphoreum	ANT-2200	142521	5.1	38.88	Scaffold	19	25	2/1	4667	2200 m
P. profundum	SS9	264698	6.4	41.70	Chromos.	3	3	2/1	5489	2551 m, associated with Amphipoda
	3TCK	177858	6.19	41.30	Scaffold	11	82	–	5549	Shallow-water
P. damselae	subsp. piscicida DI21	621318	4.77	40.16	Scaffold	56	497	1/1	–	Liver of fish
	subsp. *damdelae* CIP102761	221638	5.05	40.70	Contig	–	8	–	3528	Ulcer of fish
P. angustum	S14	177538	5.18	39.70	Scaffold	25	45	2/–	4743	Shallow-water
P. leiognathi	*lrivu* 4.1	87311	5.27	41.00	Scaffold	20	184	2/1	4296	Light organ
P. mandapamensis	svers.1.1.	278018	4.6	41.10	Scaffold	11	31	2/–	4006	Light organ
P. halotolerans	DSM 18316	60081	4.69	50.90	Scaffold	53	62	–	3943	Saline water
	svers.1.1.	18037	5.43	49.50	Contig	–	80	–	4117	Surface of a mussel
P. marin	AK15	525928	5.54	46.20	Contig	–	83	–	4904	10.5
Photobacterium	sp. SKA34	177658	4.99	39.60	Scaffold	18	88	–	4726	–
P. gaetbulicola	Gung47	304541	5.91	49.73	Chromosome	2	2	2/–	5211	Tidal flat

– undetermined

2010; Martini et al. 2013). In order to understand the evolutionary strategy developed by this strain to adapt to the deep marine environment, we sequenced its genome and carried out physiological analyses. Metabolism pathway analysis revealed a versatile growth capacity. The strain ANT-2200 lives in a place with saturated dissolved oxygen (Tamburini et al. 2013). Consistently, we identified 10 genes required for the aerobic respiration with oxygen as terminal electron accepter. Interestingly we also found genes coding for the typical anaerobic respiration enzymes and confirmed their functions by growth analysis under various conditions. Moreover, we identified four gene clusters encoding Trimethylamine *N*-oxide (TMAO) reductases. TMAO is an efficient organic osmolyte that counteracts the effects of pressure on proteins (Yancey et al. 1982). TMAO content in tissues of deep-sea animals increases with depth (Yancey et al. 2002) and its accumulation increases internal osmolarity of fish. The up-limit of tissue TMAO concentration seems to constrain the marine animals from inhabiting the deepest ocean environment (Yancey et al. 2014). TMAO also serves as an electron acceptor in bacteria for generating energy via respiration. It is plausible that TMAO released from dead fish increases its instant availability in the deep-sea habitats. We observed that addition of TMAO significantly improved the anaerobic growth of ANT-2200 and that its TMAO reductase activity is enhanced by high hydrostatic pressure, implying an important role of this enzyme in adaptation of bacteria to deep-sea habitats.

Materials and methods

Growth media and cultures

P. phosphoreum strain ANT-2200 was grown in YPG rich medium (Martini et al. 2013) or ANT-minimal medium that consists of artificial seawater supplemented with vitamins and trace elements [as described in (Frankel et al. 1997)], and HEPES (0.3 % final w/v concentration), NH_4Cl (0.2 %), K_2HPO_4 (1.86 %), Na_2MoO_4 (0.0024 %), and Na_2SeO_3 (0.0017 %). When indicated, sodium formate (0.2 %, final concentration), sodium nitrate (0.1 %), sodium fumarate (1.5 %), TMAO (0.1 %), glucose (0.2 %) or maltose (0.2 %) was added. The cultures of this mesophile, deep-sea strain were incubated anaerobically at room temperature (22–25 °C) in dark.

TMAO reductase analysis

The periplasmic fractions were prepared by osmotic-shock treatment and TMAO reductase activity was measured by enzymatic assay using benzyl viologen as an electron donor in anaerobic cuvette or visualized by activity staining using methyl viologen as an electron donor after resolving periplasmic proteins on native polyacrylamide gels as previously reported (Santini et al. 1998). The bands exhibiting activity were excised from the gels and their protein content was identified by nanoLC-ESI–MS/MS spectrometry analysis using the Ultimate 3000/LTQ Orbitrap XL instrument as described by Christie-Oleza et al. (Christie-Oleza et al. 2012).

Genome sequencing and analysis

The *P. phosphoreum* ANT-2200 whole genome was sequenced at Genoscope as previously described (Zhang et al. 2014a). The annotation was performed using the Microscope platform (https://www.genoscope.cns.fr/agc/microscope/home/index.php) (Vallenet et al. 2013) and promoter prediction was performed using Virtual Footprint version 3.0 (http://www.prodoric.de/vfp/vfp_promoter.php). Ortholog analysis has been carried out at MBGD (http://mbgd.genome.ad.jp/). The updated genome sequence has been deposited at EMBL with the accession numbers WGS: CCAR020000001-CCAR020000010.

Results and discussion

Genome overview

Using optical mapping we have updated and reassembled the draft genome of *P. phosphoreum* ANT-2200. The genome consists of chromosome I (3,293,680 base pairs), chromosome II (1,661,466 base pairs), a plasmid (113,194 base pairs) and an un-positioned scaffold (32,257 base pairs), with a total size of 5,100,597 base pairs (Fig. 1; Table 2). The *parAB* genes (PPBDW_v2_p0098/97) encoding plasmid partition proteins were found on the plasmid. The chromosome II contains a large region of 90,335 bps with predicted CDSs only on the clockwise-transcription strand (Fig. 1, at 9 o'clock direction). In this region, several exported proteins of unknown function are predicted, which are conserved among *Photobacterium* genomes. The two-chromosome composition has been found in *P. profundum* SS9, *P. mandapamensis* strain *svers.* 1.1, *P. leiognathi, P. angustum* and *P. gaetbulicola* Gung47 (Okada et al. 2005a; Urbanczyk et al. 2011; Vezzi et al. 2005) (Table 1). We have compared the chromosomes of ANT-2200 with those of *P. profundum* piezophilic strain SS9 and piezosensitive strain 3TCK using Blastn program. As shown in the Dot Plot View, the alignment of two chromosomes I from ANT-2200 and SS9 showed a main diagonal line with two inverse sections as an opposite diagonal line (Supplementary information, Figure S1, A1). The homologous regions cover 62 % of ANT-2200 chromosome I with 90 % sequence identity.

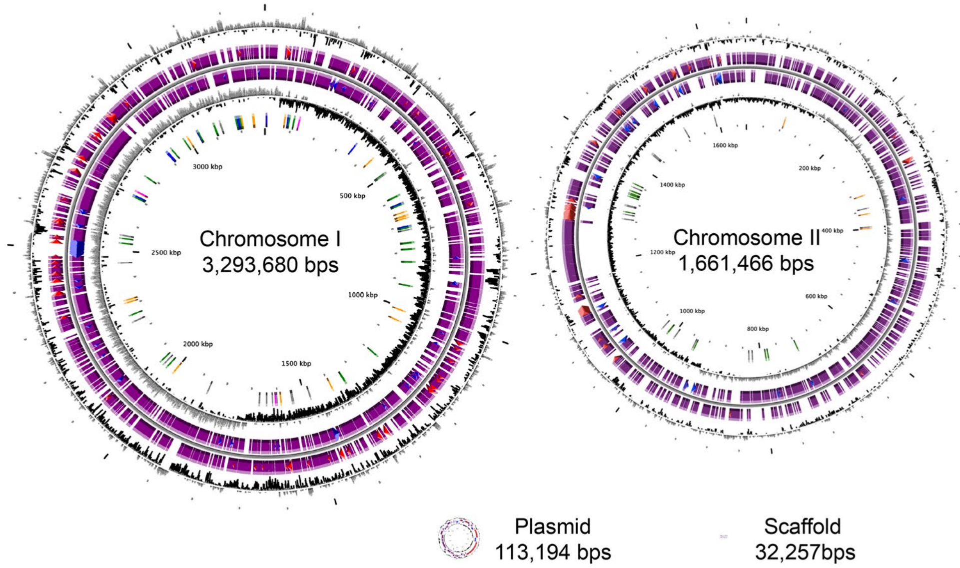

Fig. 1 Overview of *P. phosphoreum* ANT-2200 genome. Two chromosomes, the plasmid and the un-positioned scaffold are presented in proportion with to their sizes. *Circles* display (from the *outside*): (1) G + C percent deviation (GC window—mean GC) in a 1000-bp window. (2) Predicted CDSs transcribed in the clockwise direction. (3) Predicted CDSs transcribed in the counterclockwise direction. Genes displayed in (2) and (3) are *color-coded* according different categories: *red* and *blue* manually curated gene functions; *purple* primary/Automatic annotations. (4) GC skew (G + C/G-C) in a 1000-bp window. (5) rRNA (*blue*), tRNA (*green*), misc_RNA (*orange*), Transposable elements (*pink*) and pseudogenes (*grey*)

Table 2 Summary of genomic features of *Photobacterium phospheorus* ANT-2200

Characteristics	Chromosome I	Chromosome II	Plasmid	Un-positioned scaffold
Size (bp)	3,293,680	1,661,466	113,194	32,257
G + C content (%)	39.83	37.34	34.18	38.37
No. of contigs	6	1	1	2
Average CDS length (bp)	933.96	954.53	875.66	558.29
No. of CDS	3011	1477	96	41
rRNA	24	0	1	0
tRNA	126	42	1	0

The chromosomes II display only sporadic short homologous fragments (Figure S1, A2). When comparing with the draft genome of *P. profundum* piezosensitive strain 3TCK, chromosome I of ANT-2200 and the region from 2-Mbp to the end of the 3TCK genome shared sequence identity of 90 % (Figure S1, B1), while limited alignment has been observed between the ANT-2200 chromosome II and the first 2-Mbp region of the 3TCK draft genome (Figure S1, B2). Similar results were obtained between the chromosomes of *P. profundum* piezophilic strain SS9 and piezosensitive strain 3TCK (Figure S1, C1 and C2). Thus, it is possible that 3TCK genome also consists of two chromosomes. The chromosomes I and II of ANT-2200 possess 8.25 and 12.9 % coding DNA sequence (CDS) showing no homology to any previously reported sequences. Taken together, the results indicate that the chromosome I of ANT-2200 is conserved while the chromosome II is more diverse compared to those from other *Photobacterium* spp., which is consistent with the report that the chromosome I is more stable and contains the most established genes in *P. profundum* SS9 (Vezzi et al. 2005) and *Vibrionaceae* in general (Dryselius et al. 2007; Okada et al. 2005b).

Among the thirteen available genomes of *Photobacterium* spp., ANT-2200 has an average genomic size but the lowest G + C % content (Table 1). Currently only the genomes of *P. profundum* SS9 and *P. gaetbulicola* Gung47 have been completely sequenced and assembled at chromosome level, whereas those of ANT-2200 and other *Photobacterium* spp. are at either scaffold or contig levels with gaps (Table 2). Therefore, caution must be taken in functional genomic comparisons and analyses. The ANT-2200 genome encodes at least 169 tRNA genes that cover all the 20 common amino acids in addition to 1 SeC(p) tRNA for Selenocysteine (Sec, U, or Se-Cys). Twenty-four rRNA genes have been identified, all located in chromosome I, including 11 encoding 5S rRNA, 7 encoding 23S rRNA and 6 encoding 16S rRNA, while at least three more 16S rRNA genes are expected as 3 incomplete sequenced rDNA clusters are present at the end of contigs. The 16S rRNA genes of ANT-2200 shared 99.93 % identity, which is in contrast to the fifteen 16S rRNA genes from SS9 displaying 5.13 % sequence divergence (Vezzi et al. 2005).

Ortholog analysis has been performed between the genome of *P. phosphoreum* ANT-2200 and the two completely sequenced genomes of *P. profundum* SS9 and *P. gaetbulicola* Gung47. Among total 7576 ortholog clusters identified, 2686 (35.5 %) are common to all three genomes (Supplementary Information Table S1). In addition, 831 (11.0 %) and 259 (3.4 %) ortholog clusters are shared by *P. phosphoreum* ANT-2200 with *P. gaetbulicola* Gung47, or with *P. profundum* SS9, respectively. Therefore, *P. phosphoreum* ANT-2200 seems more closely related with *P. gaetbulicola* Gung47 than with *P. profundum* SS9. Among the 259 orgholog clusters shared by *P. phosphoreum* ANT-2200 and *P. profundum* SS9 but absent from *P. gaetbulicola* Gung47 about 52.9 % has been annotated as Hypothetical proteins for the genome of the strain SS9 at MBGD. Another high functional category (8.9 %) is involved in cross-membrane transport. Therefore, it is difficult to provide a clear explanation of how the two species adapt to deep-sea habitats from comparative genome analysis.

P. phosphoreum ANT-2200 is moderately piezophilic (AlAli et al. 2010; Martini et al. 2013). Adaptation to high hydrostatic pressure of deep marine biosphere has been extensively studied in the moderately piezophilic strain SS9. The *toxR/S* and *ompL/ompH* gene clusters are widely distributed in members of the family *Vibrionaceae.* Welch and Bartlett have identified mutants of the *toxR* gene and demonstrated its involvement in pressure-responsive expression of OmpL and OmpH in *P. profundum* SS9 (Welch and Bartlett 1998). We have identified the *toxR/S* (PPBDW_v2_I21883/84) and *ompH* (PPBDW_v2_I21892) within a gene cluster, and a separated *ompL* (PPBDW_v2_I30078) on the chromosome I of ANT-2200 strain. A potential pressure sensing function of the ToxR in ANT-2200 needs to be confirmed.

Besides the similarity we also observed interesting differences between the two moderately piezophilic *Photobacterium* strains, i.e. SS9 and ANT-2200. It has been reported that photo-activated photolyase genes are absent from the genome of SS9, as expected for deep-sea bacteria living in habitats without sunlight (Vezzi et al. 2005). However, we found a *phr* gene (PPBDW_v2_II0175) encoding deoxyribodipyrimidine photolyase in a synteny group conserved among *P. mandapamensis*, *P. damselae* subsp. *damselae* CIP, *Photobacterium* sp. AK15, *P. angustum* S14, *Photobacterium* sp. SKA34 and piezosensitive *P. profundum* strain 3TCK, but absent from the piezophilic strain SS9. Deletion and insertion events occurred in the region downstream of *phr* in the synteny in the compared *Photobacterium* genomes, suggesting a genomic plasticity of this cluster. It's possible that *P. phosphoreum* ANT-2200 might be in an early stage of its adaptation to deep biosphere and the vestigial *phr* gene functioning in euphotic bacteria has not been lost yet.

Flagellar apparatus

Bacterial motility and flagellar apparatus are evolved and regulated during their adaptation to different environment. Recently we reported a robust flagellar apparatus containing 7 flagella and 24 fibrils arranged into seven intertwined hexagonal arrays within a sheath (Ruan et al. 2012). Bacteria possessing such exquisite architecture are capable of circumventing and squeezing through obstacles (Ruan et al. 2012; Zhang et al. 2014b; Zhang et al. 2012), implying an advantage in their searching for nutrients at different layers of marine sediments. Flagellar composition has been proposed as a trait of adaptation to deep-sea habitats, i.e. the genomes of deep-sea piezotolerant bacterium *Shewanella piezotolerans* WP3 (Wang et al. 2008), piezophilic *P. profundum* SS9 and its deep-sea relative *P. profundum* DSJ4 (Campanaro et al. 2005; Eloe et al. 2008) possess both polar flagellar (PF) and lateral flagellar (LF) systems. In contrast, the piezosensitive strain *P. profundum* 3TCK lacks the lateral flagella (Campanaro et al. 2005). Interestingly *P. phosphoreum* ANT-2200 bears two major flagellar gene clusters, in addition to four loci encoding sodium ion-driven flagellar motor component (*pomBA*, *motY*, *motX*) and a separate *fliL2* gene (Fig. 2). Cluster I on the Chromosome I (PPBDW_v2_I21979 to PPBDW_v2_I22023) has about 45 genes and is perfectly conserved compared to the polar flagellar gene cluster of *P. profundum* SS9 and 3TCK strains (Fig. 2). A locus composed of *cheYZABW* genes upstream of *fliA* is also conserved in the three genomes (data not shown). The major difference between them is the copy number of flagellin *fliC* gene, which has a single copy in ANT-2200 PF cluster but two copies in *P. profundum*. The gene cluster II consisting of 26 flagellar genes (PPBDW_v2_p0015 to PPBDW_v2_p0050) is located on the plasmid, suggesting a possible transfer among closely related bacteria. Five loci encompassing more than two genes (loci i to v in Fig. 2) are located in different order compared to those in gene cluster I, indicating a rearrangement during the evolution of flagellar gene clusters. As in *P. profundum* SS9, *motA* and *motB* encoding a proton-driven flagellar motor reside within the LF gene cluster, *pomAB*, *moxY* and *motX* encoding sodium ion-driven motors are present at three separated loci on chromosome I of ANT-2200 (Fig. 2).

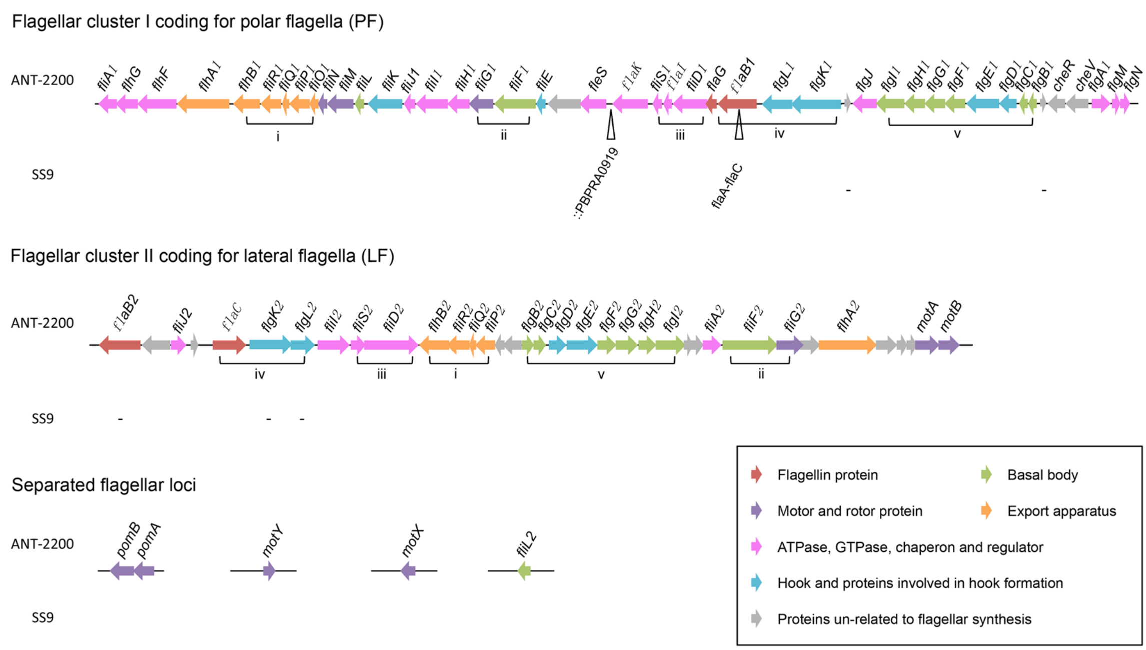

Fig. 2 Gene clusters coding flagellar systems in *P. phosphoreum* ANT-2200. Gene clusters encoding polar flagella (from PPBDW_v2_I21979 to PPBDW_v2_I22023) or lateral flagella (from PPBDW_v2_p0015 to PPBDW_v2_p0050) or loci of sodium-driven flagellar motor genes *pomAB* (PPBDW_v2_I22099 and PPBDW_v2_I22098), *motY* (PPBDW_v2_I20639) and *motX* (PPBDW_v2_I40044), or *fliL2* (PPBDW_v2_I10172, putative basal-body associated protein) are presented in order and proportionally as in the genome with the *functional colors* indicated at the *bottom-right*. The cluster I is perfectly conserved in the genome of *P. profundum* SS9 except an inserted '::PBPRA0919' gene, duplicated flagellin genes '*flaA-flaC*' and 2 genes absent from SS9 genome as indicated with *solid lines* under the corresponding genes found in the ANT-2200 genome. The gene loci conserved in cluster I and cluster II are indicated with *i*, *ii*, *iii*, *iv* and *v*

Versatile growth capacity of ANT-2200

Analysis of the genome of *P. phosphoreum* strain ANT-2200 reveals its versatile metabolic capacities. We have performed comparative analysis of MicroCyc metabolic pathways between *P. phosphoreum* ANT-2200 and *Photobacterium profundum* piezophilic strain SS9 and piezosensitive strain 3TCK at MaGe plateform. Among the 446 pathways analyzed, 249 are fully detected and 139 partially occur in ANT-2200 genome, while 239 are fully and 189 partially found in the genome of the piezophilic strain SS9 (Supplementary Information Table S2). In contrast, only 5 and 48 pathways are fully and partially detected in the partially sequenced genome of the piezosensitive strain 3TCK. Apparently more metabolic pathways were found in the partially sequenced genome of *P. phosphoreum* ANT-2200 than in the completely sequenced genome of *P. profundum* SS9. To corroborate the growth potential we analyzed its growth in minimal (oligotroph) and rich media (copiotroph) based on several metabolic pathways. The cultures were performed in dark to mimic conditions at 2200 m and at room temperature (22–25 °C) as it is a mesophile. Under anaerobic conditions bacteria derive the energy via fermentation on sugars or anaerobic respiration with organic or inorganic electron donors and acceptors. Genes encoding typical glucose phosphotransferase (PTS) systems and periplasmic binding protein dependent maltose uptake system were found in the genome of ANT-2200 (Table 3). When inoculated in the ANT-minimal media supplemented with either glucose or maltose (see "Materials and methods"), ANT-2200 grew well with maximal yield of about 0.3 absorbance at 600 nm (Fig. 3). These results confirmed the fermentation capacity of ANT-2200 on these sugars. Bacteria often use formate as an electron donor and nitrate, trimethylamine *N*-oxide (TMAO) or fumarate as electron acceptors to establish respiration chains. We found genes coding for formate dehydrogenases, nitrate reductase, TMAO reductases and fumarate reductase (Table 3). Supply of formate together with one of the three electron acceptors to minimal media sustained the growth of ANT-2200 whereas no growth was observed without formate or either electron acceptor. The low yield of biomass is probably due to poor carbon supply, and addition of fumarate increased the yield by about 50 % in comparison with those of TMAO and nitrate (Fig. 3). Both the growth rate and the maximal yield in rich media are largely increased comparing to the growth in minimal media, and addition of either the three electron acceptors in rich media could further improve the growth. Together these results show the versatile growth capacity of the strain *P. phosphoreum*

Table 3 *P. phosphoreum* ANT-2200 genes supporting fermentation, respiration and chemoorganotrophic growth analyzed in this study

CDS	Gene	Function	In *P. profundum* SS9
PPBDW_v2_I22052	*crr*	Glucose-specific enzyme IIA component of PTS, involved in catabolite repression	PBPRA0861-H[a]
PPBDW_v2_II1438	*ptsG*	PTS system, glucose-specific IIBC component	PBPRA1203-A[a]
PPBDW_v2_II1374	*malE*	Maltose transport, periplasmic maltose binding protein	PBPRA0861-H[a,b]
PPBDW_v2_I21280/79/78	*fdhABfndI*	Formate dehydrogenase	PBPRA1862/1/0
PPBDW_v2_I22058	*napC*	Periplasmic nitrate reductase, cytochrome c-type	PBPRA0854-H[a]
PPBDW_v2_I50007/8/9/10	*frdABCD*	Fumarate reductase	PBPRA3378/9/80/1
PPBDW_v2_I20849/8/7	*torECA*	Periplasmic TMAO reductase	PBPRA1467-H[a,b]
PPBDW_v2_I20985/4/3	*torCAD*	Periplasmic TMAO reductase	PBPRA1467-H[a,b]
PPBDW_v2_I21631/30/29	*torECA*	Periplasmic TMAO reductase	PBPRA1467-H[a,b]
PPBDW_v2_I20753/2	*torC-torA*	Periplasmic TMAO reductase	PBPRA1467-H[a,b]
PPBDW_v2_I20759	*torS*	Induction of TorA reductase synthesis	PBPRB0026-H[c]

The labeling "-H" and "-A" indicate that those genes are up-regulated at high hydrostatic pressure or atmosphere pressure, respectively

[a] Le Bihan et al. (2013)

[b] Vezzi et al. (2005)

[c] Campanaro et al. (2005)

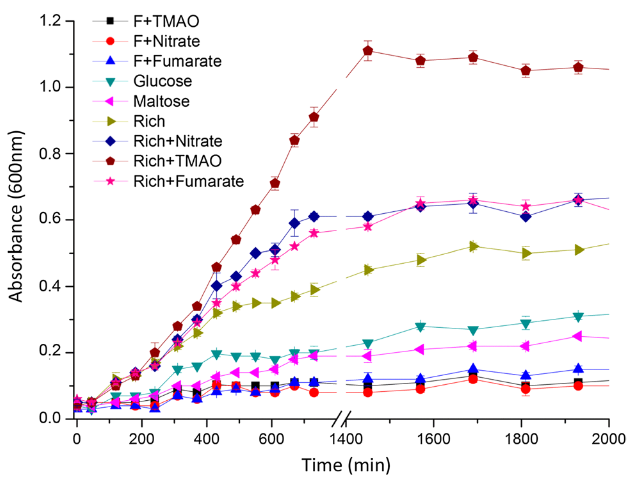

Fig. 3 Growth of *P. phosphoreum* ANT-2200 under fermentation, respiration or chemoorganotrophic conditions. *P. phosphoreum* ANT-2200 was inoculated anaerobically in minimal marine media or rich media without glycerol (Rich) supplemented with formate (F), TMAO, nitrate, glucose or maltose. There was no growth in the minimal media with formate but without electron acceptor, that was used as blank reference in the measurement of absorbance

ANT-2200 living at deep-sea habitat with sporadic inputs of various organic nutrients.

It is noticed that while addition of nitrate and fumarate to the rich media raise the maximal yield slightly (A_{600} increased from 0.5 to 0.6), addition of TMAO augmented it by around twofolds (A_{600} increased from 0.5 to 1.1), indicating that TMAO might be the most suitable electron acceptor of those tested in supporting the growth of ANT-2200.

TMAO reductase in *P. phosphoreum* ANT-2200

Anaerobic respiration of TMAO involves the reduction of TMAO into TMA (trimethylamine), which is mainly catalyzed by TMAO reductase. In *E. coli* genes responsible for the TMAO reductase synthesis are located at two loci: *torS-torT-torR-torCAD*, and *torYZ* [(Ansaldi et al. 2000; Bordi et al. 2004; Simon et al. 1995), Fig. 4]. TMAO reductase consists of a periplasmic catalytic subunit (TorA or TorZ) containing molybdo-cofactor and a membrane-anchored cytochrome C (TorC or TorY). A dedicated chaperone TorD is involved in maturation of TorA (Genest et al. 2005). The expression of *torCAD* operon is induced by TMAO via the TorS-TorR two-component system and a periplasmic TMAO-binding protein TorT in *E. coli* (Ansaldi et al. 2001). We found four loci coding for TMAO reductases on the chromosome I of *P. phosphoreum* ANT-2200 (Fig. 4). The gene composition and cistronic structure are different from those found in *E. coli*. The first locus encompasses the regulatory genes *torS-torT* (PPBDW_v2_I20759/58) and TMAO reductase *torC$_1$-torA$_1$* genes (PPBDW_v2_I20753/52). The two *tor* clusters are separated by four CDS unrelated to TMAO metabolism. Intriguingly the *torC$_1$* and *torA$_1$* are encoded by the complementary DNA strands and unlike all current known *torCA* genes that form single transcription units (Fig. 4). The second (PPBDW_v2_I20849 to PPBDW_v2_I20847) and the fourth (PPBDW_v2_I21631 to PPBDW_v2_I21629) *tor* loci on the ANT-2200 genome are composed of *torECA* gene clusters (Fig. 4). The third *torR-torC$_3$A$_3$D$_1$* locus (PPBDW_v2_I20986 to PPBDW_v2_I20983) corresponds to the canonical *torR-torCAD* gene cluster. The four TorA proteins in ANT-2200 shared identity

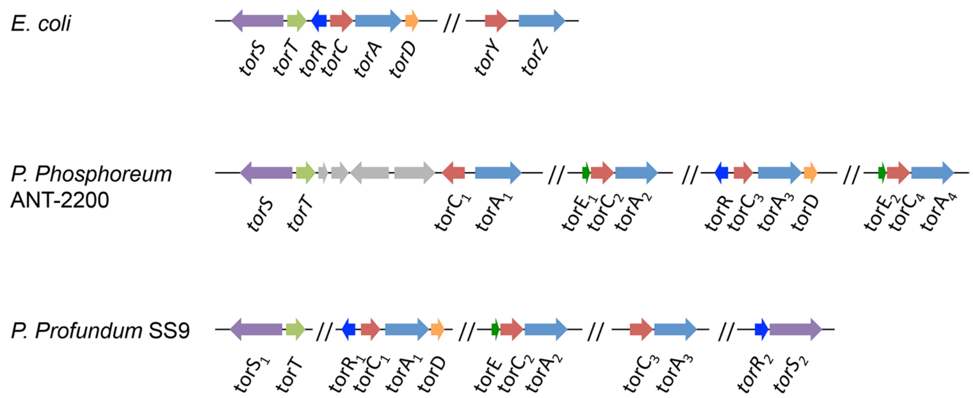

Fig. 4 Structure and composition of *tor* gene clusters for TMAO reductases. *Arrows* indicate the transcription and translation directions of the *tor* genes and *arrow lengths* are proportional to the gene sizes. Paralogous genes are indicated by the *same color* and *grey color* shows the genes unrelated to the TMAO metabolism

ranging from 36 to 72 %, suggesting differences in their function. The piezotolerant strain SS9 also carries more than one copy of TMAO reductases in its genome, including a *torR-torCAD* locus (PBPRA1497 to PBPRA1494), a *torECA* locus (PBPRA1469 to PBPRA1467), a *torCA* locus (PBPRA2364 to PBPRA2363), a *torT-torS1* cluster, (PBPRA1231 to PBPRA1232) and a $torR_2S_2$ locus (PBPRA0025 to PBPRA0026).

Enhancement of ANT-2200 TMAO reductases by elevated pressure

To assess the effect of high hydrostatic pressure on TMAO reductases in ANT-2200 we measured the TMAO reductase activity of cells grown under different conditions. The four TorA proteins of ANT-2200 possess the twin-arginine translocation (TAT) export signal peptides, and thus, should be exported into the periplasm via the TAT pathway as previously reported for TorA in *E. coli* (Santini et al. 1998). We prepared the periplasmic fractions from ANT-2200 and analyzed the TMAO reductase activities by both activity staining after resolving the proteins on native polyacrylamide gels or enzyme assay of the periplasmic fractions. TorA alone exhibits the TMAO reductase activity when benzyl viologen or methyl viologen is used as an artificial electron donor to reduce TMAO. Two bands displaying the basic activity of TMAO reductase were observed in the periplasmic fractions of ANT-2200 cells incubated at atmosphere pressure without inducer (TMAO) (Fig. 5a, lane 1). When ANT-2200 cells were incubated at 22 MPa, equivalent to the pressure at depth of 2200 m, the activity of the upper-band was enhanced while the lower band remained unchanged (Fig. 5a, lane 2). The total TMAO reductase activity increased about three-fold (Fig. 5a). When TMAO as an inducer was added in the growth media, the total activity of TMAO reductase almost doubled. Meanwhile, the intensities of both bands augmented, and a barely visible band appeared above the upper-band (Fig. 5a, lane 3). However, no additional increase of the activity was observed when both TMAO and high pressure was applied (Fig. 5a, lane 4).

We then identified TMAO reductase isoenzymes present in the upper and lower bands using a label-free shotgun proteomic procedure (Armengaud et al. 2014). Identification of a given isoenzyme was validated only when at least two specific and distinct proteotypic peptides had been detected. As shown in Fig. 5b, the upper-band contains TorA1 and TorA2 while the lower band has only TorA3. This identification was unambiguous as 34, 43 and 38 different peptide sequences were certified by tandem mass spectrometry, respectively. TorA4 has not been identified in this experiment. The normalized spectral counts allow the comparison of relative abundances of proteins between samples (Armengaud et al. 2014). When incubated at high pressure (22 MPa) TorA1 protein content increased by 3.8 folds whereas TorA2 and TorA3 only slightly increased (about 1.3 fold) compared to the cultures at atmospheric pressure. Addition of TMAO increases the TorA1 and TorA3 quantities by about 2.5 folds. TorA2 is less enhanced by elevated pressure or TMAO induction, but it is the most abundant TMAO reductases among the three isoenzymes. Therefore, TorA2 was constantly produced regardless the growth conditions.

TMAO regulates *tor* gene expression via TorR regulator that binds at TTCATA motif in the regulation regions of *tor* gene clusters (Ansaldi et al. 2000; Bordi et al. 2004; Simon et al. 1995). We found one binding site upstream of the $torC_3A_3D_1$ operon, one in the −70 to −80 region from the translation start codon of $torC_1$ and two in front of the $torE_1C_2A_2$ operon (Figure S2). Notably, transcription of *torA1* is expected in opposite direction with that of *torC1*. The presence of these putative TorR binding sites is consistent with the increase in TMAO-stimulated reductase activities. The contribution of each TorA in supporting the ANT-2200 growth and mechanism of high pressure effect on *torA* gene expression could be analyzed once genetic tool has been established for this strain.

TMAO is highly abundant in fish tissues and the content increases proportionally with the depth where fish lives in

A

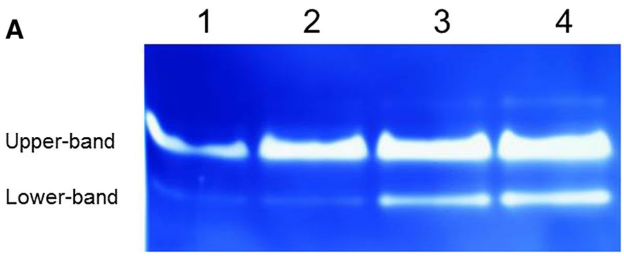

	1	2	3	4
Pressure	-	+	-	+
TMAO	-	-	+	+
Activity	1.06	2.94	1.97	2.58
Growth (A_{600})	0.59	0.37	1.32	1.40

B

	1	2	3	4
Upper-band				
TorA1	29	110	73	50
TorA2	111	146	185	114
TorA3	0	0	0	*1*
Lower-band				
TorA1	0	0	0	0
TorA2	0	0	0	0
TorA3	45	60	118	110

Fig. 5 TMAO reductase activity of *P. phosphoreum* ANT-2200. ANT-2200 cells are incubated in rich media at atmosphere pressure (−) or 22 MPa (+), without (−) or with (+) TMAO. Periplasmic fractions were resolved on 10 % native polyacrylamide gels and TMAO reductase activity was visualized by activity staining (**a**). In parallel the TMAO reductase activity was measured spectrophotometrically by following the oxidation of benzyl viologen and specific activities (μmol TMAO reduced per min per mg of proteins) are presented (**a**). The normalized spectral counts for each TorA isoenzyme identified by tandem mass spectrometry are indicated in *Panel* **b**. Notably, only the values higher than 3 are meaningful and the spectral count 1 (in *italic*) for TorA3 in the upper-band might be due to a carry-over from other samples, which can be considered as an artifact

ocean (Yancey et al. 2014). It serves as an efficient osmolyte to stabilize proteins against high hydrostatic pressure. The up-limit of the predicated isoosmotic state at 8,200 m has been considered as a biochemistry restriction that accounts for the absence of fish in the deepest 25 % of the ocean (8400–11,000 m) (Yancey et al. 2014). In parallel, transcriptome analysis showed that high pressure up-regulates the transcription of several genes involved in TMAO metabolism in *P. profundum* piezophilic strain SS9, including a TMAO sensor gene *torS* (Campanaro et al. 2005) and structural genes of TMAO reductase (subunit TorA) (Le Bihan et al. 2013; Vezzi et al. 2005). In addition, high pressure up-regulates the expression of protein TnaA tryptophanase that probably plays a role in counter-balancing the putative alkalinization due to trimethylamine reduction (Le Bihan et al. 2013). We identified the counterparts of these pressure up-regulated genes, except *tnaA*, in the genome of *P. phosphoreum* ANT-2200. Interestingly, among the three TMAO reductase isoenzymes of ANT-2200 we found that only TorA1 was significantly enhanced by elevated pressure at protein and enzymatic activity levels. In addition, simultaneous application of high hydrostatic pressure and TMAO did not produce an accumulative effect on the total TMAO reductase activity. Instead, it was even slightly reduced in comparison to sole application of pressure (Fig. 5). The pressure enhancement of TorA1 isoenzyme is thus dissociated from the induction and utilization of TMAO, suggesting it might be synthesized constantly in deep-sea piezosphere to quickly react to release of TMAO from fish in pervasive and changing gradients of nutrients.

Microorganisms adapt to the high hydrostatic pressure by various strategies, e.g. increasing polyunsaturation of membrane fatty acids, switching respiratory chains in energy metabolism and controlling gene expression via multiple regulatory systems (ToxS/R, OmpH/L, RecD) (Abe et al. 1999). Our genomic analysis confirmed the occurrence of these regulators in the deep-sea luminous strain ANT-2200 and revealed the highest copy number of gene clusters encoding TMAO reductases in bacteria. Biochemistry study showed the enhanced TMAO reductase activity under elevated hydrostatic pressure. Proteomic analysis corroborated the enhancement and further pointed out the increase of isoenzyme TorA1 as the major contribution to the activity augmentation. Together these results suggest that increasing TMAO reductase-coding gene copies and the enzymatic activity might be a strategy developed by bacteria to adapt to the deep-sea habitats where TMAO content increases with depth. Moreover, TMAO metabolism represents a novel model to shed light on molecular mechanism that governs the adaptation of microorganisms to the piezosphere.

Acknowledgments This work was supported by Grants SIDSSE-201307, SIDSSE-QN-201405, SIDSSE-QN-201406 and SIDSSE-QN-201408 from Sanya Institute of Deep-Sea Sciences and Engineering, the Strategic Priority Research Program grant XDB06010203 and International Partnership for Innovative Team Program (20140491526) from the Chinese Academy of Sciences, the NSFC 41506147 from National Natural Science Foundation of China, a grant for LIA-BioMNSL from Centre National de la Recherche Scientifique, the grant DY125-15-R-03 from China Ocean Mineral Resources R & D Association (COMRA) Special Foundation, the Grant NSFC 41306161 from the National Science Foundation of China and a grant from Mt. Tai Scholar Construction Engineering Special Foundation of Shandong Province. We acknowledge France Genomique for the support for this sequencing project.

References

Abe F, Kato C, Horikoshi K (1999) Pressure-regulated metabolism in microorganisms. Trends Microbiol 7:447–453

AlAli B, Garel M, Cuny P, Miquel JC, Toubal T, Robert A, Tamburini C (2010) Luminous bacteria in the deep-sea waters near the ANTARES underwater neutrino telescope (Mediterranean Sea). Chem Ecol 26:57–72

Ansaldi M, Simon G, Lepelletier M, Mejean V (2000) The TorR high-affinity binding site plays a key role in both *torR* autoregulation and *torCAD* operon expression in *Escherichia coli*. J Bacteriol 182:961–966

Ansaldi M, Jourlin-Castelli C, Lepelletier M, Theraulaz L, Mejean V (2001) Rapid dephosphorylation of the TorR response regulator by the TorS unorthodox sensor in *Escherichia coli*. J Bacteriol 183:2691–2695

Armengaud J, Trapp J, Pible O, Geffard O, Chaumot A, Hartmann EM (2014) Non-model organisms, a species endangered by proteogenomics. J Proteomics 105:5–18

Ast JC, Dunlap PV (2005) Phylogenetic resolution and habitat specificity of members of the Photobacterium phosphoreum species group. Environ Microbiol 7:1641–1654

Bordi C, Ansaldi M, Gon S, Jourlin-Castelli C, Iobbi-Nivol C, Mejean V (2004) Genes regulated by TorR, the trimethylamine oxide response regulator of *Shewanella oneidensis*. J Bacteriol 186:4502–4509

Campanaro S et al (2005) Laterally transferred elements and high pressure adaptation in *Photobacterium profundum* strains. BMC Genomics 6:122

Christie-Oleza JA, Fernandez B, Nogales B, Bosch R, Armengaud J (2012) Proteomic insights into the lifestyle of an environmentally relevant marine bacterium. ISME J 6:124–135

Dryselius R, Kurokawa K, Iida T (2007) Vibrionaceae, a versatile bacterial family with evolutionarily conserved variability. Res Microbiol 158:479–486

El-Hajj ZW, Allcock D, Tryfona T, Lauro FM, Sawyer L, Bartlett DH, Ferguson GP (2010) Insights into piezophily from genetic studies on the deep-sea bacterium, *Photobacterium profundum* SS9. Ann N Y Acad Sci 1189:143–148

Eloe EA, Lauro FM, Vogel RF, Bartlett DH (2008) The deep-sea bacterium *Photobacterium profundum* SS9 utilizes separate flagellar systems for swimming and swarming under high-pressure conditions. Appl Envionment Microbiol 74:6298–6305

Frankel RB, Bazylinski DA, Johnson MS, Taylor BL (1997) Magneto-aerotaxis in marine coccoid bacteria. Biophys J 73:994–1000

Genest O, Ilbert M, Mejean V, Iobbi-Nivol C (2005) TorD, an essential chaperone for TorA molybdoenzyme maturation at high temperature. J Biol Chem 280:15644–15648

Le Bihan T, Rayner J, Roy MM, Spagnolo L (2013) *Photobacterium profundum* under pressure: a MS-based label-free quantitative proteomics study. PLoS One 8:e60897

Martini S et al (2013) Effects of hydrostatic pressure on growth and luminescence of a moderately-piezophilic luminous bacteria *Photobacterium phosphoreum* ANT-2200. PLoS One 8:e66580

Okada K, Iida T, Kita-Tsukamoto K, Honda T (2005a) Vibrios commonly possess two chromosomes. J Bacteriol 187:752–757

Okada K, Iida T, Kita-Tsukamoto K, Honda T (2005b) Vibrios commonly possess two chromosomes. J Bacteriol 187:752–757

Ruan J et al (2012) Architecture of a flagellar apparatus in the fast-swimming magnetotactic bacterium MO-1. Proc Natl Acad Sci USA 109:20643–20648

Santini CL, Ize B, Chanal A, Muller M, Giordano G, Wu LF (1998) A novel sec-independent periplasmic protein translocation pathway in *Escherichia coli*. EMBO J 17:101–112

Simon G, Jourlin C, Ansaldi M, Pascal MC, Chippaux M, Mejean V (1995) Binding of the TorR regulator to cis-acting direct repeats activates *tor* operon expression. Mol Microbiol 17:971–980

Tamburini C et al (2013) Deep-sea bioluminescence blooms after dense water formation at the ocean surface. PLoS One 8:e67523

Urbanczyk H et al (2011) Genome sequence of Photobacterium mandapamensis strain svers.1.1, the bioluminescent symbiont of the cardinal fish Siphamia versicolor. J Bacteriol 193:3144–3145

Vallenet D et al (2013) MicroScope–an integrated microbial resource for the curation and comparative analysis of genomic and metabolic data. Nucleic Acids Res 41:D636–D647

Vezzi A et al (2005) Life at depth: *Photobacterium profundum* genome sequence and expression analysis. Science 307:1459–1461

Wang F et al (2008) Environmental adaptation: genomic analysis of the piezotolerant and psychrotolerant deep-sea iron reducing bacterium *Shewanella piezotolerans* WP3. PLoS One 3:e1937

Welch TJ, Bartlett DH (1998) Identification of a regulatory protein required for pressure-responsive gene expression in the deep-sea bacterium *Photobacterium* species strain SS9. Mol Microbiol 27:977–985

Yancey PH, Clark ME, Hand SC, Bowlus RD, Somero GN (1982) Living with water stress: evolution of osmolyte systems. Science 217:1214–1222

Yancey PH, Blake WR, Conley J (2002) Unusual organic osmolytes in deep-sea animals: adaptations to hydrostatic pressure and other perturbants. Comp Biochem Physiol A: Mol Integr Physiol 133:667–676

Yancey PH, Gerringer ME, Drazen JC, Rowden AA, Jamieson A (2014) Marine fish may be biochemically constrained from inhabiting the deepest ocean depths. Proc Natl Acad Sci USA 111:4461–4465

Zhang WJ et al (2012) Complex spatial organization and flagellin composition of flagellar propeller from marine magnetotactic ovoid strain MO-1. J Mol Biol 416:558–570

Zhang SD et al (2014a) Genome sequence of luminous piezophile *Photobacterium phosphoreum* ANT-2200. Genome Announc 2:e00096–14

Zhang SD et al (2014b) Swimming behaviour and magnetotaxis function of the marine bacterium strain MO-1. Environ Microbiol Rep 6:14–20